Università di Pisa

Modeling decoherence effects on the transport properties

Marco G. Pala
Dipartimento di Ingegneria dell'Informazione: Elettronica, Informatica, Telecomunicazioni, Università di Pisa
Giuseppe Iannaccone
Dipartimento di Ingegneria dell'Informazione: Elettronica, Informatica, Telecomunicazioni, Università di Pisa

M.G.Pala, G.Iannaccone, "*Modeling decoherence effects on the transport properties*", Journal Computational Electronics, **2**, pp.393-396 (2003).

Journal of Computational Electronics 2: 393–396, 2003

Modeling Decoherence Effects on the Transport Properties of Mesoscopic Devices

M.G. PALA AND G. IANNACCONE
Università degli Studi di Pisa, Dipartimento di Ingegneria dell'Informazione, via Diotisalvi 2, I-56122 Pisa, Italy

Abstract. In this paper we present a Monte Carlo technique aimed at including the effects of decoherence in mesoscopic electron transport in the scattering matrix of the system such technique is based on a phenomenological microscopic model, that captures the effect of elastic interactions in terms of a random term added to the phase of the single particle wave function. Given the random character of scattering events, each Monte Carlo run provides a particular occurrence of the reduced single particle scattering matrix. Average transport properties are obtained from large samples of Monte Carlo runs. We focus on the simulation of magnetoconductance in Aharonov-Bohm rings, and relate the amplitude of the h/e oscillations to the strength of dephasing mechanisms.

Keywords: decoherence, mesoscopic transport, dephasing length, Aharonov-Bohm ring

1. Introduction

Several aspects that make electron transport in mesoscopic systems such an interesting field of research are a consequence of the coherence of the wave function. Indeed, well known mesoscopic device concepts are essentially interferometric modulators based on the exploitation of coherent electron transport [1,2].

However, interaction of electrons with other particles like phonons or, especially at very low temperatures, other electrons [3], randomizes the phase of the single particle wave function. Dephasing suppresses quantum interference effects and is responsible for the transition from a quantum coherent to a macroscopic classical behavior.

Mesoscopic physics is located between the microscopic quantum world and the semiclassical world and is only partially affected by decoherence [4]. For these reasons, an accurate simulation of transport in mesoscopic devices would require to include a tunable degree of dephasing, in order to address the whole range of transport regimes, from purely coherent to totally incoherent.

A well known method to include dephasing in a mesoscopic device consists in adding an external voltage probe [5–7]. Alternatively, the effect of dephasing can be modeled by adding an imaginary potential to the Hamiltonian, therefore introducing a mechanism for the absorption of the coherent part of the wave function [8–10].

From our point of view, the first method has the limit of introducing a spatially localized "dephaser" that completely cancels phase memory, while the process is distributed in the device region. On the other end, the models based on absorption do not warrant continuity of the probability current density.

The dephasing length l_ϕ represents the characteristic length for loss of coherence in a mesoscopic device. It can be experimentally evaluated by measuring the weak localization correction to the conductivity [11] in semiconductor heterostructures [12], Si MOSFETs [13] and metal conductors [14]. Hansen *et al*. [15] and Pedersen *et al*. [16] estimated the phase coherence length as a function of temperature by means of the amplitude damping of Aharonov-Bohm (AB) oscillations and found an inverse proportionality of l_ϕ on the temperature in agreement with the theoretical model of [17]. The AB ring is the most convenient mesoscopic structure to investigate decoherence since it presents both purely interferometric

oscillations of the magnetoconductance with period of the magnetic flux $\Phi_0 = h/e$, weak localization effects [18] and universal conductance fluctuations [19,20].

In this paper we propose a phenomenological model for decoherence in mesoscopic devices that treats dephasing as a distributed phenomenon in the device region and ensures the conservation of probability density. A Monte Carlo procedure allows to take into account the random variation of phase occurring in the device volume due to elastic interactions. Internal parameters may be varied to adjust l_ϕ and the level of coherence of the transport regime.

2. Monte Carlo Model

The model is developed within the framework of the Landauer-Büttiker theory [21] of transport in a mesoscopic device. The conductance of a generic structure is related to the transmission probability matrix $T = tt^\dagger$ by the formula $G = ge^2/h \sum_{i,l} T_{i,l}$, where t is the transmission matrix, g is the degeneracy factor and the sum is over the all the elements of T, corresponding to the l-th injected mode and the i-th transmitted mode.

The device domain is divided into a sufficient number of slices along the propagation direction (i.e. the x-axis). The electronic wave function at the j-th slice reads

$$\psi_j(x, y) = \sum_n \frac{\mathcal{X}_{j,n}(y)}{\sqrt{|k_{j,n}|}} \left(a_{j,n} e^{ik_{j,n}x} + b_{j,n} e^{-ik_{j,n}x}\right), \quad (1)$$

where $\mathcal{X}_{j,n}(y)$ are the transverse eigenvectors with eigenenergies $E_{j,n}$ and the longitudinal wave vectors $k_{j,n}$ are related to the total energy E by the requirement $E = E_{j,n} + \hbar^2 k_{j,n}^2/2m_j$. The set of coefficients $a_{j,n}$ and $b_{j,n}$ can be obtained by imposing the continuity of the wave function and of the current density at the interface between the j-th and the $(j+1)$-th slice. The scattering matrix S relates the coefficients of the wavefunctions of the j-th and $(j+1)$-th slices as follows:

$$\begin{pmatrix} b_j \\ a_{j+1} \end{pmatrix} = S \begin{pmatrix} a_j \\ b_{j+1} \end{pmatrix} = \begin{pmatrix} r & t' \\ t & r' \end{pmatrix} \begin{pmatrix} a_j \\ b_{j+1} \end{pmatrix}, \quad (2)$$

where the symbols t, t', r and r' indicate the transmission and reflection matrices. The composition between two adjacent scattering matrices S_1 and S_2 gives a final $S = S_1 \otimes S_2$ with transmission and reflection matrices given by:

$$\begin{aligned} r &= r_1 + t_1'(1 - r_2 r_1')^{-1} r_2 t_1 \\ t &= t_2(1 - r_1' r_2)^{-1} t_1 \\ t' &= t_1'(1 - r_2 r_1')^{-1} t_2' \\ r' &= r_2' + t_2(1 - r_1' r_2)^{-1} r_1' t_2'. \end{aligned} \quad (3)$$

The total scattering matrix of the structure S_T is given by the composition $S_T = S_1 \otimes S_2 \cdots S_N$, where the symbol $\otimes$ represents the composition described in Eq. (3). The presence of a magnetic field $\mathbf{B} = B\hat{\mathbf{z}}$ perpendicular to the propagation plane xy, is taken into account adopting the transverse gauge $\mathbf{A} = Bx\hat{\mathbf{y}} = A(x)\hat{\mathbf{y}}$ for the vector potential $\mathbf{A} = \nabla \times \mathbf{B}$ as described in [22]. The new Hamiltonian is written as the sum of two terms: $H(x, y) = H_{\text{trans}}(y) + H_{\text{long}}(x)$, where $H_{\text{trans}} = [p_y - eA(x_j)]^2/2m_y + V(y)$ refers to the transversal part of the Hamiltonian and $H_{\text{long}} = p_x^2/2m_x$ to the longitudinal one. The eigenvectors are given by the product of the eigenvectors for the two Hamiltonians, that are plane waves for H_{long} and the vectors

$$\mathcal{X}_{n,j}(y) = \mathcal{X}^0_{n,j}(y) \exp[-ieA(x_j)y/\hbar] \quad (4)$$

for H_{trans}, where $\mathcal{X}^0_{n,j}(x)$ are the solutions in the case $B = 0$. Besides, using this gauge, the eigenvalues $E_{j,n}$ are unaltered by the presence of the magnetic field. We note that the condition for the validity of the discretization of H_{trans} is that the magnetic flux through a generic slice $[A(x_{j+1}) - A(x_j)]W$ is smaller that the quantum flux e/h, where W is the transverse device length.

Now we introduce in our description the effects of decoherence as a dephasing of the wave function in Eq. (1). The coherent propagation through the j-th slice is described by a diagonal transmission matrix with elements $e^{ik_{j,m}d_j}\delta_{mn}$ where $d_j = x_{j+1} - x_j$. We modify the transmission matrix adding to each diagonal term a random phase ϕ_{R} so that the generic element of the transmission matrix is

$$t_{mn} = e^{i(k_{j,m}d_j + \phi_{\text{R}})}\delta_{mn}. \quad (5)$$

ϕ_{R} is extracted by a random number generator and obeys a zero average Gaussian distribution with variance $\sigma_j^2 = d_j/l_\phi$. The larger the variance the stronger the dephasing. The scattering matrix obtained in such a way only represents a particular occurrence of the reduced scattering matrix of the single particle. The

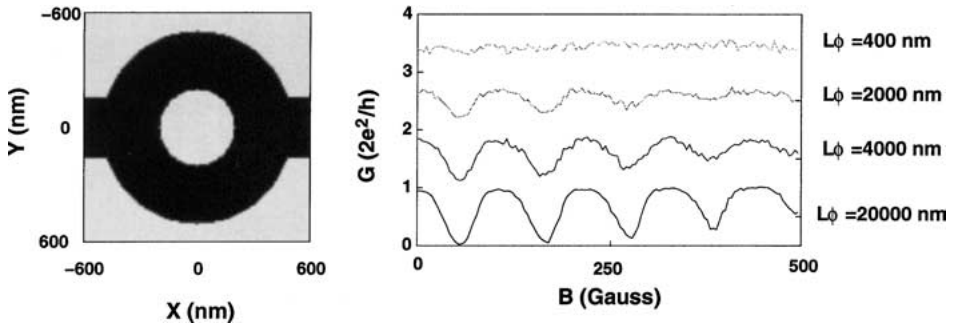

Figure 1. Left: the AB ring with internal radius of 200 nm, external radius of 500 nm and wire width of 300 nm. Right: the AB oscillations with varying degree of decoherence in the case of single mode propagation. From the top to the bottom $\sigma^2 = 5 \times 10^{-2} (l_\phi = 400$ nm), $1 \times 10^{-2} (l_\phi = 2\ \mu$m), $5 \times 10^{-3} (l_\phi = 4\ \mu$m), $1 \times 10^{-3} (l_\phi = 20\ \mu$m). Each conductance value is shifted by one conductance quantum for clarity of presentation. The Fermi energy is 10^{-4} eV and allows the transmission of a single mode in the branch.

average reduced scattering matrix is obtained by averaging the conductance over a sufficient number of runs, typically one hundred. In this way we take into account the intrinsic statistical character of the dephasing process. We emphasize that the usual properties of the scattering matrix S, like unitarity

$$SS^\dagger = I \tag{6}$$

and the Onsager-Casimir relations [23]

$$\sum_{nm} T_{nm}(\Phi) = \sum_{nm} T'_{nm}(-\Phi), \tag{7}$$

where Φ is an external magnetic flux, still hold.

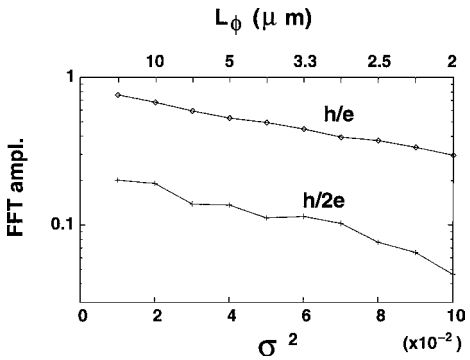

Figure 2. Amplitude of the harmonics of the magnetoconductance of period h/e and $h/2e$ with Fermi energy of 10^{-4} eV.

3. Simulation Results

In this section we apply the model to the simulation of an Aharonov-Bohm ring in the presence of decoherence and show exponential damping in the h/e and $h/2e$ oscillations.

The Aharonov-Bohm ring is characterized by pure interference and coherent effects like universal conductance fluctuations when an external gate voltage varies the Fermi energy or by weak localization effects in the magnetoconductance [18]. We have simulated a symmetric AB ring structure with internal radius of 200 nm, external radius of 500 nm, and width of the lead 300 nm. The mesh size used is 10 nm, while the number of total modes in the simulations is 20 for the case of single mode transmission.

The oscillation period can be equal to the quantum flux h/e or to the submultiples h/ne when coherent backscattering is present and the electron turns around the antidot of the ring more times. An increasing degree of decoherence suppresses the amplitude of the magnetoconductance as shown in Fig. 1. In this Figure it is possible to appreciate the transition from a coherent transport regime to a partially coherent one when the variance σ^2 of the Gaussian distribution is increased. Note that the magnetoconductance is almost unaltered for large values of the decoherence length, while is completely lost when l_ϕ is smaller than the physical size of the ring. This behavior is in agreement with the general definition of decoherence length. The considered range of values of l_ϕ, between 0.4 and 20 μm, is consistent with experimental values [15,16].

In Fig. 2 we show how to evaluate l_ϕ from the damping of different harmonics. We assume that the amplitude A_n of the h/ne harmonic is decreased according to the relation $A_n \propto e^{-nL/l_\phi}$, where L is the circumference of the ring. This behavior is confirmed by the experimental results presented in [15]. We then focus

our attention on the oscillations with period h/e. The amplitude of the harmonics of magnetoconductance show an exponential slope as a function of the variance $\sigma^2(l_\phi)$, as it is shown in the semilog plot of Fig. 2 for the cases $n = 1$ and $n = 2$. The exponential behavior is pretty clean for the h/e line.

4. Conclusion

In this paper we have described a method for modeling decoherence in mesoscopic transport that preserves probability current continuity and the distributed and statistical character of the dephasing mechanism.

The method has been applied to the simulation of magnetoconductance of an Aharonov-Bohm ring in the presence of a varying degree of scattering.

Support from IST NANOTCAD project (EC contract IST-1999-10828) is gratefully acknowledged.

References

1. F. Sols, M. Macucci, U. Ravaioli, and K. Hess, *Appl. Phys. Lett.*, **54**, 350 (1989).
2. S. Datta and B. Das, *Appl. Phys. Lett.*, **56**, 665 (1990).
3. B.L. Altshuler, A.G. Aronov, and D. Khmelnitskii, *J. Phys. C*, **15**, 7367 (1982).
4. C.W.J. Beenakker and H. van Houten in *Solid State Physics*, vol. 44, *Semiconductor Heterostructures and Nanostructures* (Academic Press, San Diego, 1991) p. 1.
5. M. Büttiker, *Phys. Rev. B*, **33**, 3020 (1986).
6. P.W. Brouwer and C.W.J. Beenakker, *Phys. Rev. B*, **55**, 4695 (1997).
7. C.W.J. Beenakker, *Rev. Mod. Phys.*, **69**, 731 (1997).
8. G. Czycholl and B. Kramer, *Solid State Comm.*, **32**, 945 (1979).
9. K.B. Efetov, *Phys. Rev. Lett.*, **74**, 2299 (1995).
10. E. McCann and I.V. Lerner, *J. Phys. Condens. Matt.*, **8**, 6719 (1996).
11. E. Abrahams, P.W. Anderson, D.C. Licciardello, and T.V. Ramakrishnan, *Phys. Rev. Lett.*, **42**, 673 (1979).
12. B.J.F. Lin, M.A. Paalanen, A.C. Gossard, and D.C. Tsui, *Phys. Rev. B*, **29**, 927 (1984).
13. D.J. Bishop, R.C. Dynes, and D.C. Tsui, *Phys. Rev. B*, **26**, 773 (1982).
14. P. Mohanty, E.M.Q. Jariwala, and R.A. Webb, *Phys. Rev. Lett.*, **78**, 3366 (1997).
15. A.H. Hansen, A. Kristensen, S. Pedersen, C.B. Sørensen, and P.E. Lindelof, *Phys. Rev. B*, **64**, 045327 (2001).
16. S. Pedersen, A.H. Hansen, A. Kristensen, C.B. Sørensen, and P.E. Lindelof, *Phys. Rev. B*, **61**, 5457 (2000).
17. G. Seelig and M. Büttiker, *Phys. Rev. B*, **64**, 245313 (2001).
18. A.B. Altshuler, A.G. Aronov, and B.Z. Spivak, *JETP Lett.*, **33**, 94 (1981).
19. A.B. Altshuler, *JETP Lett.*, **41**, 648 (1985).
20. P.A. Lee and D.A. Stone, *Phys. Rev. Lett.*, **55**, 1622 (1985).
21. D. Landauer, *IBM J. Res. Dev.*, **1**, 233 (1957); M. Büttiker, *Phys. Rev. Lett.*, **57**, 1761 (1986).
22. M. Governale and D. Boese, *Appl. Phys. Lett.*, **77**, 3215 (2000).
23. L. Onsager, *Phys. Rev.*, **38**, 2265 (1931); H.B.G. Casimir, *Rev. Mod. Phys.*, **17**, 343 (1945).
24. S. Datta, *Electronic Transport in Mesoscopic Physics* (Cambridge University Press, Cambridge, 1995), p. 17.